ISSN 0040-5795, Theoretical Foundations of Chemical Engineering, 2023, Vol. 57, No. 4, pp. 549–562. © Pleiades Publishing, Ltd., 2023.
Russian Text © The Author(s), 2023, published in Teoreticheskie Osnovy Khimicheskoi Tekhnologii, 2023, Vol. 57, No. 4, pp. 479–492.

A Hybrid Membrane for the Simultaneous Selective Sorption of Cesium in the Ionic and Colloid Forms

I. I. Vinogradov[a, b, *], E. V. Andreev[a], N. S. Yushin[a], A. S. Sokhatskii[a], V. A. Altynov[a], M. V. Gustova[a], T. N. Vershinina[a, b], I. Zin'kovskaya[a], A. N. Nechaev[a, b], and P. Yu. Apel'[a]

[a] *Joint Institute for Nuclear Research, Dubna, Moscow oblast, 141980 Russia*
[b] *Dubna State University, Dubna, Moscow oblast, 141980 Russia*
**e-mail: Ily7345@gmail.com*

Received April 10, 2023; revised April 26, 2023; accepted May 20, 2023

Abstract—The possibility for the synthesis of a hybrid membrane incorporating a track membrane as a support and a layer of chitosan fibers modified by functional groups selectively sorbing cesium is studied. The layer of chitosan fibers is formed by electromolding. The surface of the nanofibers is modified by copper and potassium ferrocyanide immobilization. The structure of the nanofiber layer modified by copper and potassium ferrocyanide is studied by scanning and transmission electron microscopy and X-ray diffraction analysis. The specific pure water production capacity of the hybrid membrane is much lower as compared to the original track membrane. The data on the sorption capacity of the copper and potassium ferrocyanide layer on the surface of the nanofibers for cesium ions are correlated with literature data. The resulting hybrid membrane is suitable for the simultaneous selective sorption of cesium in the ionic and colloid forms.

Keywords: hybrid membrane, track membrane, nanofiber, chitosan, potassium ferrocyanide, sorption, cesium

DOI: 10.1134/S0040579523040498

INTRODUCTION

As a result of human technogenic activity, synthetic radionuclides enter the environment, becoming a component of the natural world alongside natural radionuclides. Their uncontrolled migration through the hydrographic network is a factor of serious environmental danger [1]. Thus, the ^{137}Cs isotope is one of the hazardous technogenic radionuclides due to its high radioactivity and ability to substitute potassium in biochemical processes. A major fraction of cesium ions is adsorbed on the surface of colloid particles of different composition [2], and the highest coefficients of ^{137}Cs accumulation from the environment are typical of freshwater basins [3]. To remove ^{137}Cs from natural and sewage water, different methods and technological approaches have been developed [4–7]. One of the efficient methods for the removal of cesium ions is ion-exchange chromatography on the sorbents containing ferrocyanide complexes of transition metals [8]. The supports or supporting structures of ferrocyanide complexes may be ion-exchange resins, silica gels, zeolites, zirconium hydroxides, activated charcoal, and chitosan [9]. As a rule, all the above-described composite sorbents are shaped as grains. The use of materials based on chitosan as an efficient biodegradable sorbent as a supporting structure deserves particular attention. The application of ion-exchange technologies for the removal of cesium ions is efficient within a broad range of concentrations, but has a number of shortcomings, which are described in sufficient detail in the papers [10–19]. However, the application of membrane sorption technologies may be rather promising for the complex solution of the problems of removing the dissolved cesium ions from natural ecosystems, when they are present in trace quantities and adsorbed on different colloids of natural origin.

In the papers [20, 21], the authors of this paper have demonstrated that the combination of a track membrane (TM) and a chitosan nanofiber layer may become an efficient method for the production of new hybrid membranes (HMs) [22]. In continuation of this series of papers, an approach to the creation of a hybrid membrane capable of simultaneous selective sorption of cesium in the ionic and colloid forms has been proposed. Thus, the approach to the creation of a hybrid membrane prototype composed of several functional layers is schematized in Fig. 1. A microfiltration track membrane acts as a membrane separator of colloid particles and/or bacteria and hydrobionts with cesium ions adsorbed on their surface [2, 23]. A large-pore filtration nanofiber layer from chitosan and a ferrocyanide complex must provide the selective sorption of trace quantities of cesium ions dissolved in

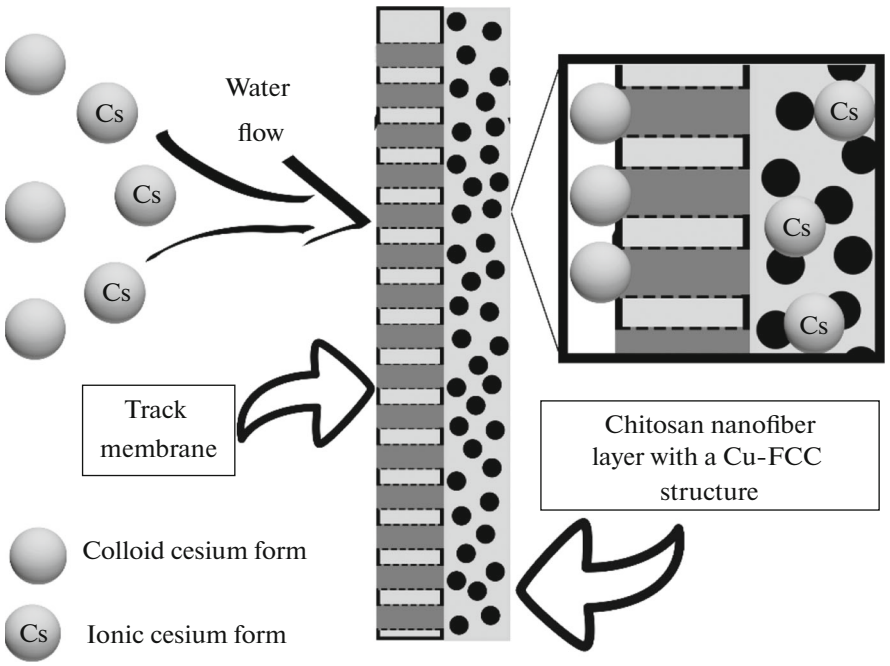

Fig. 1. Holdup of cesium in the ionic and colloid forms in in the process of filtration through the hybrid membrane.

water [24]. The metallization of the membrane with an electroconductive titanium layer strengthens adhesion between the membrane surface and the chitosan fibers. For this purpose, a polyethylene terephthalate (PET) TM was metallized with titanium by the method of magnetron sputtering [25]. The major component of the nanofibers—chitosan—provides the efficient sorption of transition metals including copper due to its polysaccharide nature [26]. Copper acts as a link between chitosan and potassium ferrocyanide $K_4[Fe(CN)_6]$ for the formation of an immobilized copper–potassium ferrocyanide complex (FCC) (Cu-FCC). As shown in [10, 15, 16, 19], this type of sorbent has a high selectivity to cesium ions. In the framework of the presented concept, it is also possible to create a much more complex three-layered structure (a nanofiber layer between two track membranes). The formation of a three-layered hybrid membrane will increase the sorbent volume and the time for the sorption of cesium ions in the hybrid membrane and, as a consequence, improve its selectivity. It should also be pointed out that, depending on the practical problem and separation process organization (dead-end or tangential filtration), the liquid flow to be separated may be fed to a two-layered membrane from the side of both the TM (see Fig. 1) and the nanofiber layer.

Therefore, the goal of this study was to create and investigate a hybrid matrix prototype capable of the simultaneous selective sorption of cesium ions in the ionic and colloid forms. To achieve this goal, it was necessary to solve a number of problems. First, it was necessary to demonstrate the possibility of the formation of a ferrocyanide complex on the surface of chitosan fibers, to study the structure and phase composition of this complex, and to prove that Cu-FCC is able to sorb cesium ions. Second, it was necessary to study the physicochemical and performance characteristics of the resulting hybrid membrane.

EXPERIMENTAL

A microfiltration TM manufactured from a Hostaphan RNK polyethylene terephthalate film (Mitsubishi Polyester Film, Germany) was used. The nominal film thickness was 23 μm, the density of the pores was $(2.7 \pm 0.3) \times 10^8$ cm^{-2}, and the diameter of the pores was 0.3 μm. Titanium was sputtered onto the track membrane on an UMN-180 extended magnetron sputter with a planar cathode (JSC Ivtekhnomash) as described in [25]. The coating was deposited from a vertically installed target by sputtering titanium with a purity of 99.7% in an argon atmosphere (99.99%). The layer thickness was 80 ± 4 nm. Hereinafter, the membranes with a deposited titanium layer are denoted as TM + Ti.

The reagents used for the formation of a FCC modified chitosan nanofiber layer were the following: Chitosan (M_w = 200000 g/mol, Bioprogress, Russia), polyethylene oxide (PEO) (M_w = 300000 g/mol, Sigma-Aldrich, Germany), glacial acetic acid (CH_3COOH, M = 60.05 g/mol, PanReac AppliChem, Barcelona, Spain), a 50-% glutaric aldehyde solution (Smart Chemistry, Russia), deionized water with a specific resistance of 18.2 MΩ cm (Milli-Q Advantage A10, Millipore), copper sulfate pentahy-

Table 1. Mass composition of the hybrid matrix per 1 cm^2

m_1, mg/cm^2, HM	m_2, mg/cm^2, TM + Ti	m_3, mg/cm^2, CS	m_4, mg/cm^2, Cu-FCC	S, cm^2/cm^2, CS
3.78 ± 0.14	3.09 ± 0.03	0.350 ± 0.001	0.34 ± 0.11	55 ± 6

drate ($CuSO_4 \cdot 5H_2O$, M = 249.68 g/mol, PanReac AppliChem, Barcelona, Spain), potassium ferrocyanide ($K_4[Fe(CN)_6] \cdot 3H_2O$, M = 422.39 g/mol, Areolab, Russia, Moscow), and cesium chloride 99.9 (CsCl, M = 168.36 (extra pure 17-2), JSC Khmikraft, Russia, Kaliningrad).

The nanofibers were formed by using a 4% chitosan solution and PEO (at a mass ratio of 90/10) in 90% acetic acid [27, 28].

The electromolding of a chitosan nanofiber layer on TM + Ti was carried out on a Nanon-01A setup (MECC Co. LTD, Japan). A F90KhSh200 mm drum collector (size 29.7 × 21 cm) was selected as an electrode. Sputtering was performed in the following mode: voltage, 28 kV; solution dosing rate, 1 mL/h; die size, 0.210 mm; die–electrode distance, 15 cm; die–electrode angle, 90°; drum collector rotation speed, 50 rpm; die velocity along axis X, 1 cm/s; sputtered solution volume, 5 mL ($m_{portion}$ = 0.2 g). This sputtered solution volume was determined as optimal. It has been experimentally established that attempts at increasing the sputtered solution volume lead to deformation in the nanofiber layer during its modification with copper–potassium ferrocyanide due to the appearance of mechanical stresses and delamination from TM + Ti. The electromolding regime was selected in the previous papers [21]. Hereinafter, the thus-formed membrane is denoted as TM + Ti + CS.

The freshly molded chitosan nanofiber layer quickly degrades in an aqueous medium. To stabilize the nanofiber layer and prevent its degradation, it was subjected to thermal and chemical crosslinking in compliance with the recommendations given in the papers [29, 30]. The thermal treatment of the specimens was performed in a drying cabinet at a temperature of 120°C for 1 h [30]. The membrane specimens subjected to thermal treatment have the abbreviation TEMP in their names. Chemical crosslinking was carried out in glutaric aldehyde vapor in a vacuum drying cabinet. An aqueous solution of 25% glutaric aldehyde (GA) with a volume of 10 mL was placed into a vacuum drying cabinet to the membrane specimens (temperature, 37°C; vacuum pressure, 3×10^{-3} mbar; chemical crosslinking time, 24 h (according to the paper [29])). The membrane specimens subjected to chemical treatment in glutaric aldehyde have the abbreviation GA in their names.

The copper–potassium ferrocyanide complex was formed in two stages by analogy with the method described in the RF patent 2430777 C1 [24]. To obtain an "anchor" in the form of copper ions on the chitosan surface, the nanofiber layer crosslinked as described above was modified in an aqueous 0.025 M $CuSO_4$ solution for 1 h. Afterwards, the specimen was washed with distilled water for 5 min, dried, and immersed into an aqueous 0.28 M $K_4[Fe(CN)_6]$ solution for 1 h 30 min. To remove unconverted compounds, the specimens were washed with distilled water for 5 min. As a result of modification, copper–potassium ferrocyanide (hereinafter, Cu-FCC) was formed on the nanofiber layer surface. The analysis of the structure and chemical composition is given below in the section RESULTS AND DISCUSSION. The mass of the hybrid membrane (m_1) and its individual components, namely, the titanium-containing track membrane (m_2), chitosan (m_3), and copper–potassium ferrocyanide (m_4), per 1 cm^2 of membrane are given in Table 1. The rightmost column contains the surface area (S) calculated for the chitosan fibers from the mass m_3, the statistically average fiber diameter (~176 ± 10 nm), and the chitosan density (1.28 g/cm^{-3}) [31].

The structure and properties of the hybrid membrane were studied by the methods described below. Scanning electron microscopy (SEM) was used for surface morphology analysis and the study of the HM cross sections. The images in the mode of secondary electrons were taken on a Hitachi S-3400N microscope at an accelerating voltage of 15 kV and further processed in the Gatan Digital Micrograph environment. The crystal structures of the material were studied in the annular dark field mode on a Thermo Scientific Talos F200i S/TEM transmission electron microscope (TEM) with an accelerating voltage of 200 kV. The analysis of the functional groups on the surface was carried out on a Nicolet iS20 IR Fourier transform spectrometer (Thermo Fisher Scientific) with the use of a Smart iTX attachment. Measurements were performed with a resolution of 4.0 cm^{-1} and the number of scans was no less than 32. IR spectra were processed in the Origin 2017 software package. The elemental composition of the specimens was studied by X-ray photoelectron spectroscopy (XPS) on a K-Alpha spectrometer (Thermo Scientific, United States) equipped with a semi-spherical analyzer. Photoelectrons were excited by X-rays from an aluminum cathode (AlK_α = 1486.6 eV) at a tube voltage of 12 kV and an emission current of 3 mA. Calibration was carried out against the C1s peak (285.0 eV) [25]. Panoramic spectra were recorded at a transmission window of 100 eV with a step of 0.5 eV. The recording and processing of the spectra were performed by the Avantage software.

The concentration of Cs ions in the sorption material volume was determined by X-ray fluorescence (XRF) analysis on a S2 PUMA desktop energy-dispersive X-ray fluorescence spectrometer (Bruker Optik GmbH) as communicated in the earlier paper [32].

X-ray diffraction studies were performed on a PANalytical EMPYREAN powder diffractometer in CuK_α radiation with a wavelength of 1.5406 Å. X-ray diffraction patterns were recorded within an angular range $2\theta = 5°–60°$ with a step of 0.02°. The phase composition was determined by using the PDF-4 database.

The adsorption capacity of the chitosan nanofibers for copper ions was determined by immersing a hybrid matrix specimen of 40 mm in diameter into a 0.025 M $CuSO_4$ solution (10 mL) for 1 h at a temperature $T =$ 296 K. After 1 h, the solution absorption spectrum was recorded in the region from 500 to 900 nm on an Evolution 600 UV-VIS spectrometer. The $CuSO_4$ concentration after sorption was determined from the calibrating curve of absorption at a wavelength of 800 nm that was plotted within a range of 0.001–0.025 M.

The absorption capacity q (mg/m^2) was calculated from the mass balance by the equation

$$q = \frac{V(C_i - C_f)}{S}, \quad (1)$$

and the sorption coefficient K_d (%) was determined from the equation

$$K_d = \frac{C_i - C_f}{C_i} \times 100\%, \quad (2)$$

where C_i is the concentration before sorption, mg/L; C_f is the concentration after sorption, mg/L; V is the solution volume, L; and S is the hybrid membrane surface area, m^2.

The kinetics and isotherm for the adsorption of cesium ions by the hybrid matrix were determined by immersing specimens of 40 mm in diameter into a CsCl solution (10 mL; 10^{-3} M, 5×10^{-4} M, 10^{-4} M, 5×10^{-5} M, 10^{-5} M). The number of parallel experiments was no less than five; the results were used to find the average value and estimate the random error. After 1, 3, 5, 10, 30, 60, and 180 min, the specimens were taken out of the solution. The concentration of cesium ions in the solution was determined by inductively coupled plasma atomic emission spectroscopy (ICP-AES) on a PlasmaQuant PQ 9000 Elite spectrometer (Analytik Jena, Germany). The line with a wavelength of 894.347 nm was selected as the analytical line. The experimental data were approximated with the Langmuir equation

$$q = q_\infty \frac{KC}{1 + KC}, \quad (3)$$

where q_∞ is the ultimate absorption capacity, mg/m^2; K is the adsorption coefficient; and C is the solution concentration.

The permeability of the specimens for water was measured in the dead-end mode by using Millipore filtration cells at a pressure of deionized water from 0.02 to 0.06 MPa with a step of 0.01 MPa. The pressure was applied from the side of the membrane modified with nanofibers.

To determine the zeta potential, the membranes were placed into an electrostatic cell with silver/silver-chloride electrodes. A potassium chloride (KCl) solution with a concentration of 0.01 M was used. Surface recharge was determined by using potassium chloride solutions with pH of 3, 5, 7, and 9. The solution was acidified with hydrochloric acid and alkalified with a KOH solution. The solution pressure was from 0.02 to 0.06 MPa. The zeta potential of the membranes was calculated by the Helmholtz–Smoluchowski equation [33].

For ease of reading, the authors have introduced the following elements in the notations of synthesized structures: "+" for an additional layer and "/" for intermediate membrane treatment.

RESULTS AND DISCUSSION

Surface Morphology of the Hybrid Membrane

A slice from the titanium metallized microfiltration track membrane with chitosan and PEO-based nanofibers deposited by electromolding is shown in Fig. 2. The membrane was manufactured by the method described in the experimental section. The microphoto presents a specimen slice with the maximum possible thickness of the fiber layer. It has been experimentally established that, under the conditions of molding on the Nanon-01A setup, it is possible to sputter no more than 0.2 g of dry chitosan–PEO mixture into the membrane surface area of 620 cm^2.

The formation of Cu-FCC on the surface of the nanofiber layer from thermally and GA crosslinked chitosan was monitored by scanning electron microscopy. Electron microphotos were taken before (Figs. 3a and 3d) and after (Figs. 3c and 3f) modifying of the nanofiber layer with ferrocyanide. The microphotos of the nanofiber layer after the sorption of copper ions are shown in Figs. 3b and 3e.

It has been established that the modification of the thermally crosslinked nanofiber layer (Fig. 3d) modified with ferrocyanide leads to the destruction of nanofibers and the formation of a monolith layer covering the track membrane surface (Fig. 3f). This effect is associated with a high rate of nanofiber destruction in an aqueous medium [34]. When studying the stability of the nanofiber layer, it has been established that, at 37°C after three days, thermally crosslinked nanofibers are subjected to hydrolytic destruction, while in the case of chemically crosslinked nanofibers this takes seven days. The first stage of destruction in the

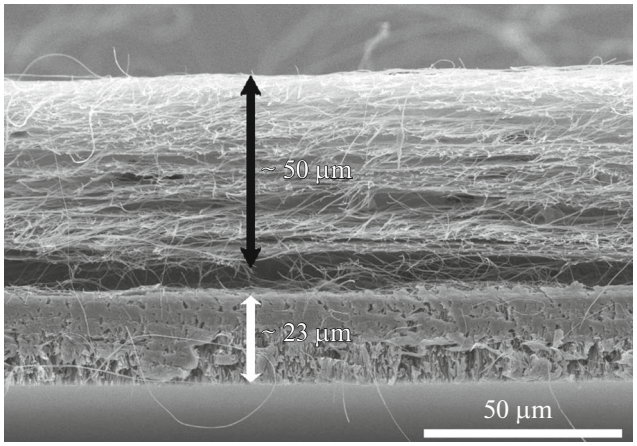

Fig. 2. Microphoto of a TM + Ti + CS slice (black bidirectional arrow is the chitosan fiber layer, and white bidirectional arrow is TM + Ti).

nanofiber layer can be visually observed after as little as 1 h of copper sorption from a 0.025 M $CuSO_4$ solution (Fig. 3e).

The modification of the GA crosslinked nanofiber layer by means of ferrocyanide results in the formation of Cu-FCC complexes on the surface of the nanofibers (Fig. 3c). The complexes appear as "lamellae" of ~500 nm in size that are chaotically arranged over the entire length of the nanofibers (Figs. 3c and 3f). Copper sorption does not lead to any visible changes in the nanofibers (Fig. 3b). Hence, to create a hybrid membrane, the chitosan nanofiber layer must be crosslinked by means of glutaric aldehyde.

The microstructure of the nanofiber layer with Cu-FCC was studied by transmission electron microscopy. In view of the specific methodological features inherent in this method (the specimen thickness must not exceed 100 nm), the specimens were manufactured by depositing the chitosan nanofiber layer onto standard grids (3 mm) with a mesh size of 200 × 200 μm. Afterwards, the grids with the nanofiber layer were modified by the method described in the experimental part. The TEM images in "light field" are shown in Fig. 4. In the images taken at a "low" magnification (Fig. 4a), it can be seen that Cu-FCC nonuniformly impregnates the nanofibers. In the region with a maximum concentration of Cu-FCC, its conglomerates are similar to a single crystal permeated by nanofibers (Fig. 4b).

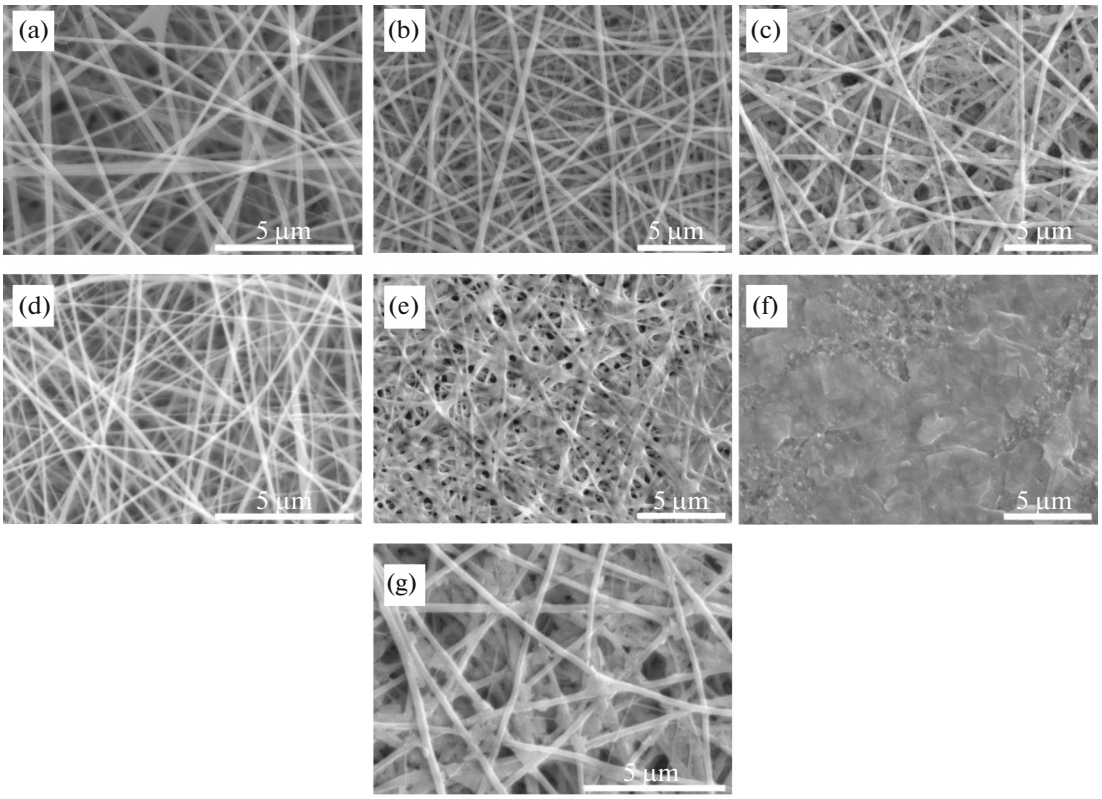

Fig. 3. Microphoto of the surface of the hybrid TM + Ti + CS membrane at different stages of modification: (a) after treatment with glutaric aldehyde, (b) after treatment in copper sulfide pentahydrate, (c) after modifying of the nanofibers with copper–potassium ferrocyanide (magnification, ×6.00k), (d) after thermal crosslinking, (e) after treatment in copper sulfide pentahydrate, (f) after modifying of the nanofibers with copper–potassium ferrocyanide, (g) after modifying of the nanofibers with copper–potassium ferrocyanide (magnification, ×10.0k).

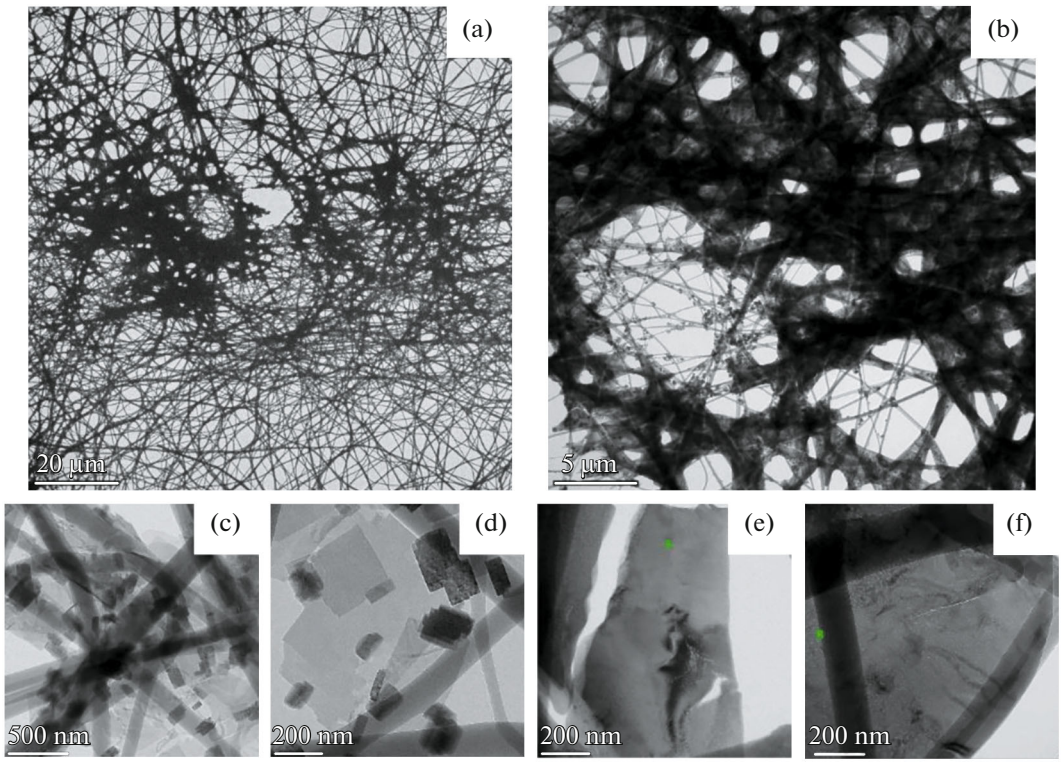

Fig. 4. TEM photos of TM + Ti + CS/GA + Cu-FCC at (a, b) low and (c, d, e, f) high magnification.

At a high magnification, the picture is radically changed. Thus, it can be observed in Figs. 4c and 4d how the Cu-FCC conglomerates form isolated crystals of 50–500 nm in size. On the contrary, the Cu-FCC in Figs. 4e and 4f resemble a single crystal. It seems that the formed Cu-FCC in Figs. 4e and 4f is not polycrystalline, as it has no sharp boundaries and domains (grains). Moreover, a porous structure is also observed in the synthesized Cu-FCC single crystal (Figs. 4e and 4f).

The microdiffraction pictures from the Cu-FCC crystals shown in Figs. 4c, 4d and 4e, 4f are presented in Fig. 5. The electron microdiffraction picture recorded for individual crystals (Figs. 5a and 5b) shows that their structure has the signs of a cubic unit cell with a lattice parameter $a \approx 10$ Å. However, the same pictures also confirm that the Cu-FCC structure is a tetragonal system. This is evidenced, in particular, by the fact that the microdiffraction pictures contain crystallographic planes 001, 021 (Fig. 5a), and 112 (Fig. 5b), which are forbidden in the cubic $K_2Cu[Fe(CN)_6]$ structure described by Rigamonti [35].

The microdiffraction pictures of the Cu-FCC single crystals (Figs. 5c and 5d) show that the structures of some crystals are different (Figs. 5a and 5b). Thus, a number of individual crystals (Figs. 5a and 5b) have a single-crystal structure that is triclinic in nature, but not the known triclinic $K_2Cu[Fe(CN)_6]$ structure described in [36]. Another interesting feature in the Cu-FCC unit cell (Figs. 5e and 5d) is the six-layered stacking of certain atomic planes. Based on TEM analysis, it is possible to conclude that the chitosan fibers are amorphous and the Cu-FCC structure has the two phases described above.

Chemical and Structural Analyses of Cu-FCC on the Nanofiber Layer Surface

Using the method of IR Fourier spectroscopy with a Smart iTX attachment, the functional groups on the surface of the chitosan were identified after modification with copper–potassium ferrocyanide (Fig. 6). The IR Fourier spectrum of the specimen TM + Ti + CS/GA is shown in Fig. 6a. A similar analysis of the functional groups on this membrane is given in the papers [21, 37]. The IR Fourier spectrum of the specimen TM + Ti + CS/GA + Cu-FCC is shown in Fig. 6b. This spectrum contains pronounced peaks at 2096 cm^{-1} (–C≡N) and 2042 cm^{-1} (–C≡N). The peak at 2096 cm^{-1} (–C≡N) corresponds to $K_2Cu[Fe(CN)_6]$. The hypsochromic shift of the wavenumber of this peak (–C≡N) is caused by the especially strong interaction between the copper atom and the –C≡N ligand due to the ability of Cu^{2+} to get electrons from the –CN group to acquire the $3d^{10}$ configuration [38, 39]. The peak at 2042 cm^{-1} (–C≡N) also corresponds to $K_2Cu[Fe(CN)_6]$, and its appearance is caused by the effect of the matrix from chitosan as a strong agent of

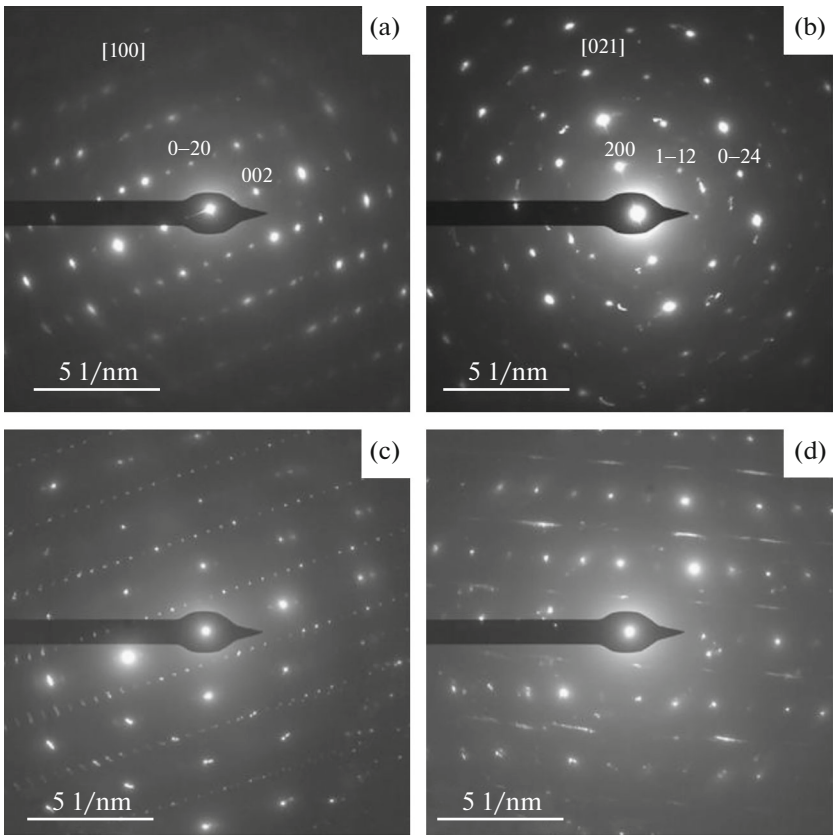

Fig. 5. Electron microdiffraction pictures for Cu-FCC crystals in TM + Ti + CS/GA + Cu-FCC: isolated (a, b) crystallites and (c, d) single crystals.

complexing with copper [40]. The peak at 1610 cm^{-1} corresponds to the bending vibrations of the hydroxyl groups of the water molecules, both crystallization and adsorbed ones [41].

According to the data [42, 43], chitosan has high sorption activity with respect to transitional metals and, to a higher extent, to copper ions. The major active sorption sites are hydroxyl and amino groups. Therefore, during the modification of the crosslinked nanofiber layer in a 0.025 M $CuSO_4$ solution for 1 h, chitosan fibers adsorbed copper ions to form chelate complexes [26]. The copper ions contained in the chelate complexes with chitosan act as a linking bridge between chitosan and potassium ferrocyanide and form Cu-FCC by an exchange reaction (Fig. 7) [40].

To confirm the sorption of copper ions, the sorption capacity of the thermally and GA crosslinked specimens TM + Ti + CS was studied. The analysis of the sorption kinetics of copper ions has shown that the thermally and GA crosslinked specimens TM + Ti + CS have sorption capacity of 127 ± 1 and 16 ± 1 mg/m^2, respectively. This difference may be due to the nanofiber layer crosslinking mechanism. Since the molding solution contains acetic acid, thermal treatment leads to the formation of acetamide (chitin) substituents in the chitosan macromolecules [37]. In the process of chemical crosslinking, the aldehyde groups of glutaric aldehyde enter the reaction with the amino groups of chitosan to give the water-insoluble form of chitosan nanofibers [29]. Hence, the decrease in the number of free amino and hydroxyl groups of chitosan worsens the ability of chitosan to form chelate bonds with copper. Therefore, it is possible to conclude that the formation of the monolith layer covering the TM + Ti surface that was communicated by us above may be caused not only by the chitosan destruction rate, but also by the formation of excessive Cu-FCC.

The quantitative control of the presence of copper, potassium, iron, carbon, oxygen, and nitrogen ions necessary for the formation of Cu-FCC was performed by X-ray photoelectron spectroscopy (XPS). Analysis was carried out on the side of the fiber layer. The TM + Ti + CS/GA/Cu^{2+} spectrum is shown in Fig. 8b, where the copper peaks (Cu2*p*3 and Cu3*p*) were revealed, indicating that copper was sorbed from the $CuSO_4$ on the nanofibers. In the same specimen, sulfur (S2*p*) and titanium (Ti2*p*) traces were revealed. The TM + Ti + CS/GA + Cu-FCC spectrum is shown in Fig. 8c. In this spectrum, all the earlier visible elements were revealed, and potassium (K2*p*) and iron (Fe2*p*) were added, confirming the presence of all the elements necessary for the formation of Cu-FCC.

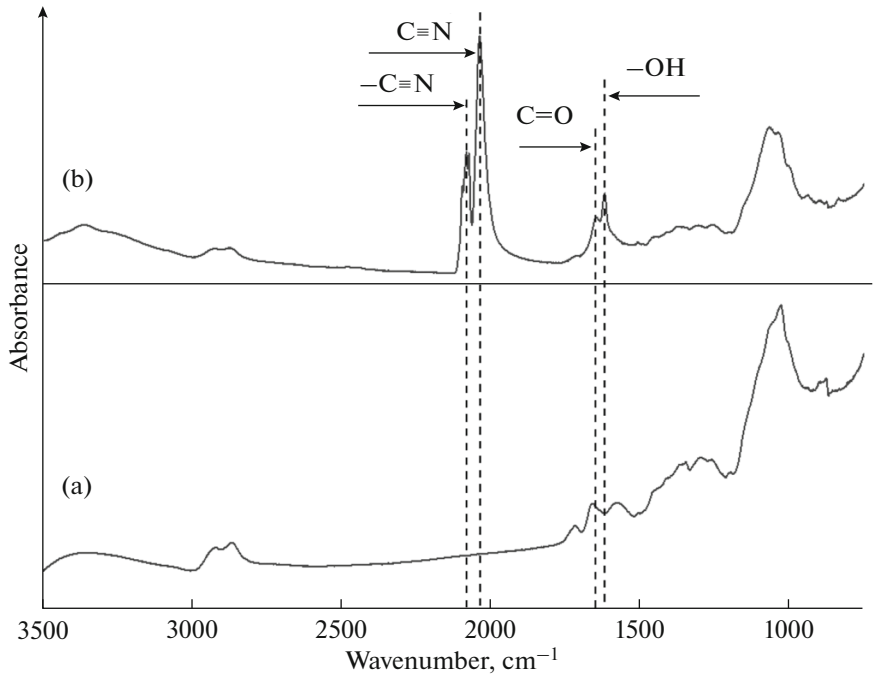

Fig. 6. IR Fourier spectra of (a) TM + Ti + CS/GA and (b) TM + Ti + CS/GA + Cu-FCC.

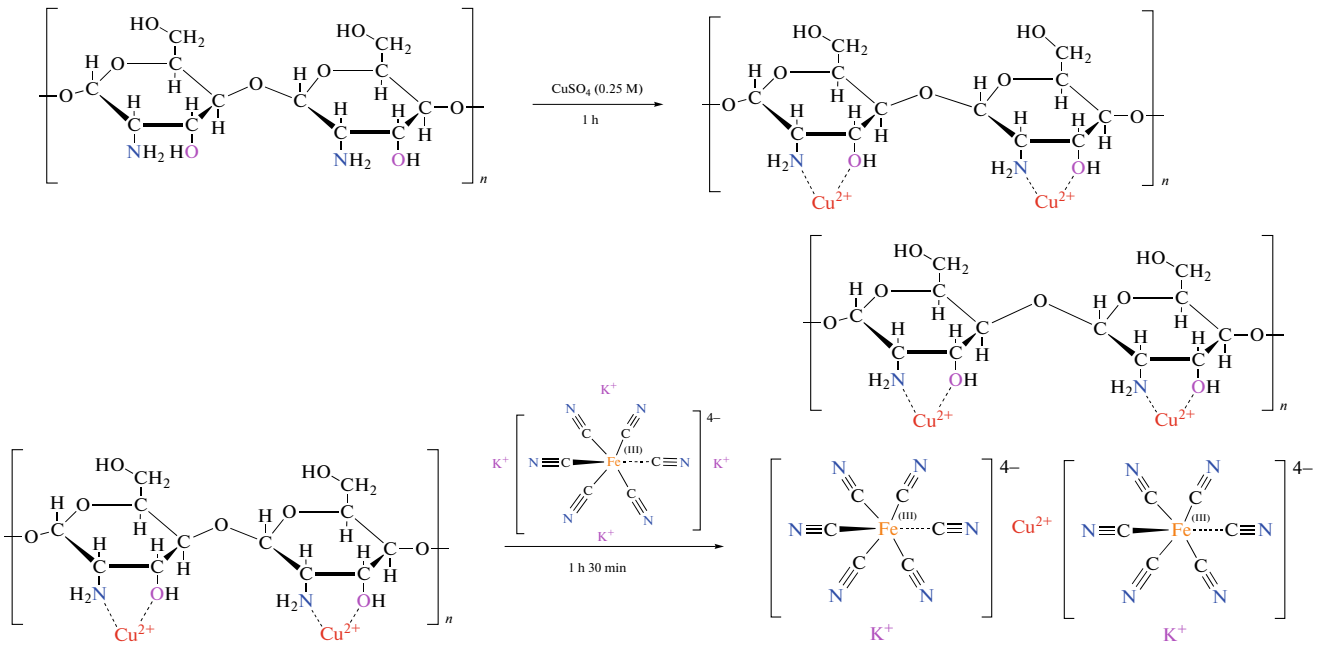

Fig. 7. Scheme for the formation of Cu-FCC on chitosan fibers for $_2Cu_3[Fe(CN)_6]_2$ as an example.

In addition, the quantitative control of the hybrid matrix for the presence of cesium ions after the contact of the specimens with a CsCl solution (10^{-5} M CsCl; $T = 296$ K; $t = 60$ min) was carried out by X-ray photoelectron spectroscopy. In Fig. 8c, the sorbed cesium peaks (Cs2*p*3, Cs3*d*5, Cs4*s*, Cs4*p*, and Cs4*d*) were added, confirming that the material has sorption activity with respect to cesium ions. The quantitative characteristics of the sorption properties of the hybrid membrane will be considered below.

Using X-ray diffraction, it has been established that the phase composition of the hybrid TM + Ti + CS/GA + Cu-FCC membrane is different than that of the TM + Ti + CS/GA (Fig. 9). The angles $2\theta = 16.9°$,

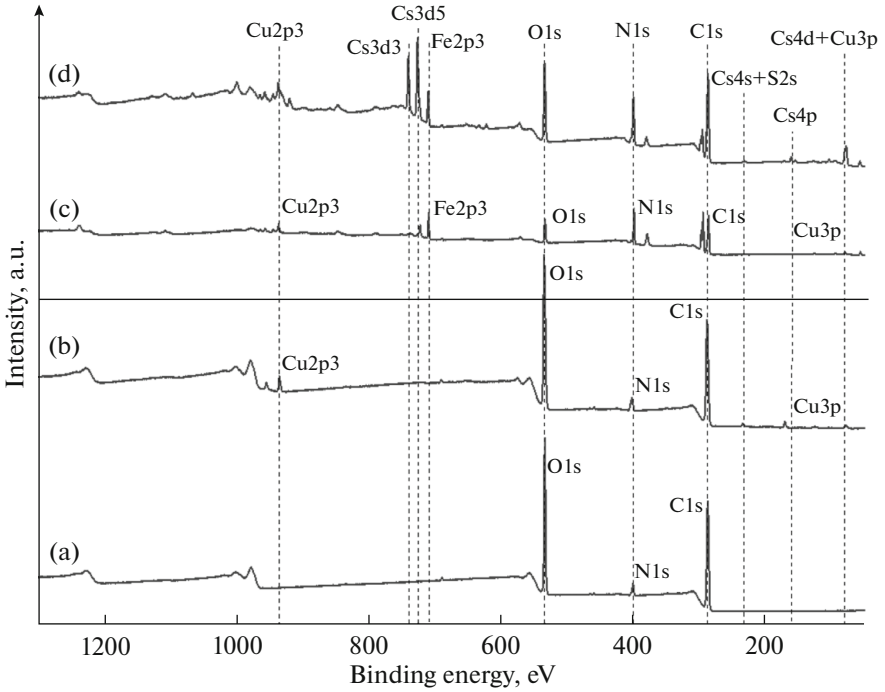

Fig. 8. XPS spectra of (a) TM + Ti + CS/GA, (b) TM + Ti + CS/GA/Cu^{2+} ($C(CuSO_4)$ = 0.025 M; T = 296 K; t = 60 min), (c) TM + Ti + CS/GA + Cu-FCC, (d) TM + Ti + CS/GA + Cu-FCC with sorbed cesium ions ($C(Cs^+) = 10^{-5}$ M; T = 296 K; t = 60 min).

18.0° and 34.2°, 36.4° correspond with an acceptable accuracy to the crystallographic planes 002, 200 and 004, 400 of the $K_2Cu[Fe(CN)_6]$ phase, which has a tetragonal unit cell with parameters a = 9.85 Å and c = 10.50 Å according to [44]. The Jahn–Teller distortion also demonstrates the splitting of diffractions 200 and 400 (2θ = 17.7° and 35.9°, Cu$K\alpha$) for the cubic $K_2Cu[Fe(CN)_6]$ crystal structure (a = 9.99 Å) due to small deformation in its unit cell [35]. Although the $K_2Cu[Fe(CN)_6]$ peaks are low in intensity and are hardly distinguishable against the background of the diffraction picture from the PET and chitosan with a maximum 2θ = 25.85° [45], it may be concluded that TM + Ti + CS/GA + Cu-FCC incorporates this phase.

Membrane-Sorption Characteristics of the Hybrid Membrane

Since we declare the synthesized material as a membrane-sorption one, the specific pure water production capacity, the surface charge, and the sorption ability with respect to cesium ions are highly important parameters.

The specific pure water production capacity was measured for TM + Ti, TM + Ti + CS/GA, and TM + Ti + CS/GA + Cu-FCC (Fig. 10a). (Let us recall that the weight of dry chitosan on TM + Ti of format A4 with a surface area of 620 cm^2 was 0.2 g, and the sputtered layer thickness, according to the slice microphotos (Fig. 2) was ~50 μm). The specific production capacity (W) of TM + Ti was found to be 0.74 ± 0.08 L/(h cm^2) at a pressure of 0.06 MPa. The specific productivity of the TM + Ti + CS/GA and TM + Ti + CS/GA + Cu-FCC was estimated as 0.67 ± 0.06 and 0.53 ± 0.05 L/(h cm^2), respectively, indicating a slight decrease in the specific production capacity as compared to the original TM + Ti. The decrease in the specific production capacity occurs due to the partial clogging of the pores and the propensity of the nanofibers toward swelling in water.

Electrokinetic measurements in the membranes make it possible to determine the isoelectric points and the sign of the charge on their surface. The hybrid Tm + Ti + CS/GA membrane has a set of both acid (–COOH, –OH) and base ($-NH_2$) groups and is amphoteric. The modification of this material with copper–potassium ferrocyanide must change the sign of the charge and the position of the isoelectric point.

The dependence of the zeta potential of TM + Ti, TM + Ti + CS/GA, and TM + Ti + CS/GA + Cu-FCC on pH is shown in Fig. 10b. The surface charge of TM + Ti + CS/GA grows as compared to TM + Ti, shifing the isoelectric point towards the acid region (pI = 3.2). This change occurs due to an increase in the number of acid groups. After TM + Ti + CS/GA is modified with copper–potassium ferrocyanide, the surface charge decreases and the isoelectric point turns back to the initial value of TM + Ti (pI = 4.5).

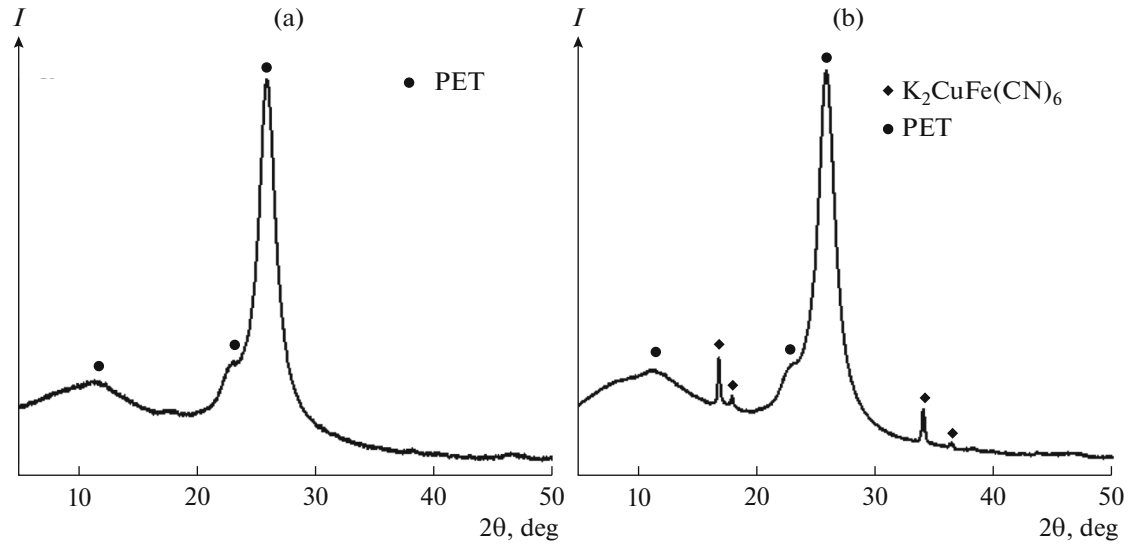

Fig. 9. X-Ray diffraction patterns of (a) TM + Ti + CS/GA and (b) TM + Ti + CS/GA + Cu-FCC.

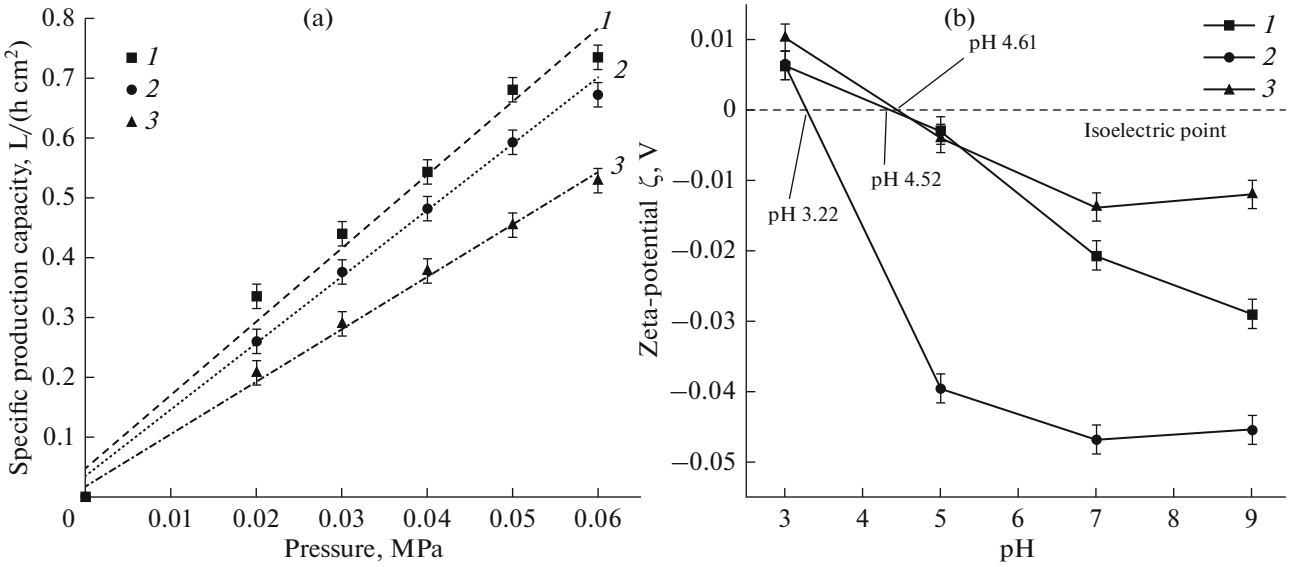

Fig. 10. (a) Average water permeability and (b) zeta potential versus pH of electrolyte: (*1*) TM + Ti, (*2*) TM + Ti + CS/GA, (*3*) TM + Ti + CS/GA + Cu-FCC.

Therefore, after the nanofiber layer is modified with copper–potassium ferrocyanide, the chitosan surface is blocked with Cu-FCC, resulting in a decrease in the surface charge.

Investigating the adsorption of cesium ions is the main goal of this study. Let us recall that the main purpose of this material is capacity for the simultaneous selective sorption of cesium in the ionic and colloid form. According to the concept proposed by the authors (Fig. 1), colloid particles of 0.3 μm in size with adsorbed cesium ions are arrested by microfiltration TM + Ti [23]. The cesium ions which have not been sorbed on colloid particles are arrested by the nanofibers from chitosan modified with copper–potassium ferrocyanide, which sorbs cesium ions by means of ion exchange.

To determine the time at which the sorption of cesium ions on the studied hybrid membrane attains a plateau, the kinetics of cesium sorption from a 0.001 M CsCl solution was studied (Fig. 11a). The quantity of cesium remaining in the solution was determined by inductively coupled plasma optical emission spectroscopy (ICP-AES). The sorption of cesium ions after 60 min attained 91% from the ultimate sorption by the Langmuir equation.

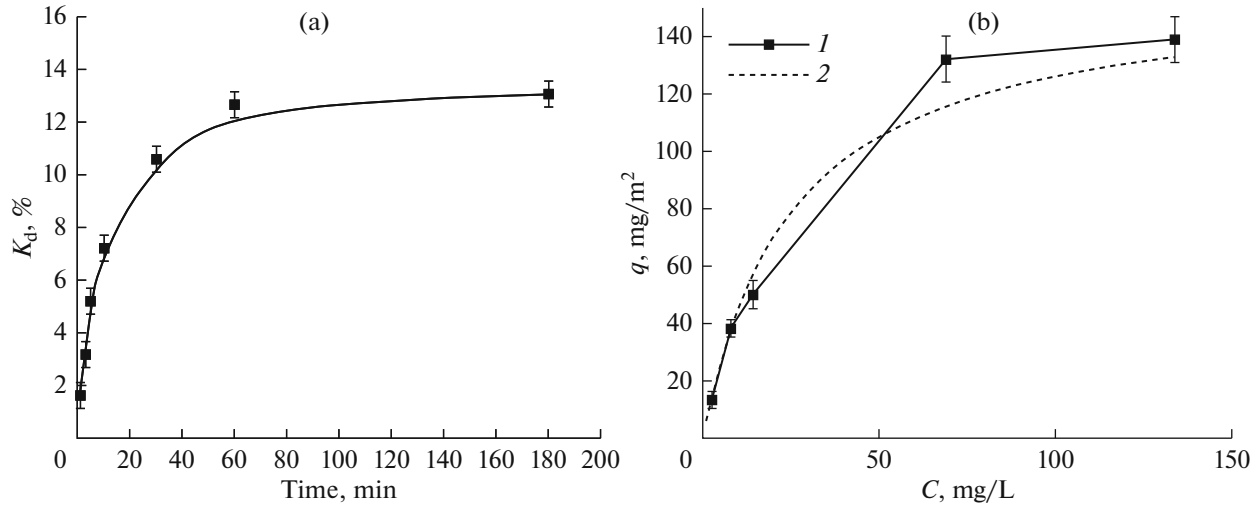

Fig. 11. (a) Kinetics of cesium ion adsorption from a 0.001 M CsCl solution on TM + Ti + CS/GA + Cu-FCC according to ICP-AES data; (b) isotherms of cesium ion adsorption from CsCl solutions on TM + Ti + CS/GA + Cu-FCC: (*1*) experimental ($T = 296$ K; $t = 60$ min), (*2*) approximation of experimental data by the Langmuir equation.

To determine the sorption capacity of TM + Ti + CS/GA + Cu-FCC, the adsorption isotherm of Cs^+ ions was measured (Fig. 11b). It has been experimentally established that TM + Ti + CS/GA sorbs less than 0.001 mg/m^2 of the cesium ions and, therefore, we considered copper–potassium ferrocyanide as a basic sorbent. The adsorption capacity (q) of the hybrid membrane was estimated as 13.4 ± 1.1 mg/m^2 ($C(Cs^+) = 10^{-5}$ M; $T = 296$ K). The sorption coefficient (K_d was equal to 65% for a 10^{-5} M CsCl solution (T = 296 K). Confirmation that cesium ions were sorbed by the synthesized hybrid membrane are given in the XPS spectra (Fig. 8d). As a result of approximation for Cs^+ adsorption on TM + Ti + CS/GA + Cu-FCC (Fig. 11b), it has been revealed that the experimental data can be satisfactorily described by the Langmuir equation. The ultimate adsorption capacity (q_∞) is 158 ± 15 mg/m^2. The found ultimate adsorption capacity correlates with the data [15, 46]. Thus, for instance, the authors [46] propose an approach to the synthesis of colloidally stable sorbents for the removal of cesium ions. Latex particles functionalized with ferrocyanides of transitional metals were applied as a basis. This type of sorbent has an ultimate adsorption capacity of 44.6 mg/g for cesium ions. A composite sorbent was synthesized in [15] on the basis of spherically grained chitosan modified with copper–potassium ferrocyanide. This type of sorbent has an ultimate adsorption capacity of 42.3 mg/g for cesium ions. For comparison, we recalculated the ultimate adsorption capacity of copper–potassium ferrocyanide on the nanofiber layer surface with respect to cesium ions, obtaining 42 ± 14 mg/g. Hence, it is possible to conclude that fiber sorbents may be quite competitive in terms of sorption capacity with the spherically grained chitosan-based sorbents modified with copper–potassium ferrocyanide. All the above-given data were measured in a binary cesium chloride solution (pH 5.6). For the additional confirmation of the efficiency of sorption of cesium ions on the synthesized hybrid membranes, it is necessary to study the effect of the ionic strength, the pH of the medium, and the presence of impurity ions. These studies are beyond the scope of the current paper and will be covered in subsequent studies.

CONCLUSIONS

Summarizing the results of the study on the creation of experimental hybrid membrane specimens for the selective sorption of cesium ions and the retention of cesium in the colloid form, it is possible to make a number of preliminary conclusions. The concept of creating a hybrid membrane that consists in combining a traditional microfiltration track membrane and a nanofiber layer from chitosan modified with copper–potassium ferrocyanide is technically implementable. High adhesion between the nanofiber layer formed by electromolding and the membrane surface is provided by an electroconductive metallic layer. Titanium, inert in the aqueous media, was selected as the metal and it was deposited by the method of magnetron sputtering. The titanium and nanofiber layer deposition processes can be implemented by roll technologies, which is an important condition for scaling the technological process for the manufacturing of hybrid membranes. The chitosan nanofiber layer was modified by copper–potassium ferrocyanide. It has been established that ferrocyanide complexes are not formed on the track membrane surface and thus the selective membrane structure remains untouched. It has been shown that

to create a hybrid matrix, the nanofiber layer thickness must be less than 50 μm. At larger nanofiber layer thicknesses, the formed ferrocyanide complex layer leads to mechanical deformations in the original track membrane. The specific pure water production capacity of the hybrid membrane is only slightly lower as compared to the value for TM + Ti. The study of the structure and morphology of the hybrid membrane by a broad spectrum of analytical methods (SEM, TEM, XPS, X-ray diffraction, IR Fourier spectroscopy) proves that copper–potassium ferrocyanide is incorporated into the hybrid matrix. The ability of the hybrid matrix to sorb cesium ions from aqueous solutions is the ultimate adsorption capacity equal to 158 ± 15 mg/m^2. This proves the correctness of the methodological approaches to the modification of the chitosan nanofiber layer with copper–potassium ferrocyanide that were earlier applied for the creation of spherically grained sorbents.

The objective function of the developed hybrid matrix is the removal of cesium in the ionic and colloid forms from aqueous media without the use of reverse osmosis or ultrafiltration. In connection with the formulated problem, further study is planned for the performance characteristics (production capacity, selectivity) of the developed hybrid membranes in the model solutions containing both free cesium ions and inorganic silica particles with cesium ions adsorbed on their surface. In the framework of the presented concept, it is planned to create a more complicated structure in the form of a "sandwich" (which represents two hybrid membranes stacked together such that their fiber layers are oriented to each other). The creation of a three-layered hybrid membrane may be necessitated by the following factors. Thus, when filtration occurs from the TM side, some pressure drop will be accounted for by the fiber layer, from which fiber and ferrocyanide particles with adsorbed cesium may be detached. The time it takes the medium with cesium ions to pass through the nanofiber layer for filteration is short. The creation of a "sandwich" will make it possible to increase the sorbent volume and the time for the sorption of cesium ions and, as a consequence, improve its selectivity. The proposed approach to the creation of microfiltration hybrid membranes will broaden the capabilities of the technologies for the removal of radionuclides from the hydrographic network.

NOTATIONS

C	concentration, mg/L
C_i	concentration before sorption, mg/L
C_f	concentration after sorption, mg/L
m	mass, mg
P	pressure, MPa
q	adsorption capacity, mg/m^2
q_∞	ultimate adsorption capacity, mg/m^2
S	hybrid membrane surface area, m^2
T	temperature, K
t	time, min
V	solution volume, L
ζ	zeta-potential, V

REFERENCES

1. Korenkov, I.P., Kiselev, S.M., Shandala, N.K., and Lashchenova, T.N., *Osnovy radioekologicheskogo i gigienicheskogo monitoring okruzhayushchei sredy* (Fundamentals of Radioecological and Hygienic monitoring of the Environment), Il'in, L.A. and Samoilov, A.S., Eds., Moscow: GEOTAR-Media, 2021.
2. Kalmykov, S.N., Migration of radionuclides through geochemical barriers, *Cand. (Chem.) Dissertation*, Moscow, Mosk. Gos, Univ., Khim. Fak., 2000.
3. Vasilenko, I.Ya. and Vasilenko, O.I., Radioactive cesium, *Energ.: Ekon. Tekh. Ekol.,* 2001, no. 7, pp. 16–22.
4. Khulbe, K.C. and Matsuura, T., Removal of heavy metals and pollutants by membrane adsorption techniques, *Appl. Water Sci.*, 2018, vol. 8, no. 1, pp. 1–30. https://doi.org/10.1007/s13201-018-0661-6
5. Sharma, S. and Bhattacharya, A., Drinking water contamination and treatment techniques, *Appl. Water Sci.*, 2017, vol. 7, no. 3, pp. 1043–1067. https://doi.org/10.1007/s13201-016-0455-7
6. Samstag, R.W., Ducoste, J.J., Griborio, A., Nopens, I., Batstone, D.J., Wicks, J.D., Saunders, S., Wicklein, E.A., Kenny, G., and Laurent, J., CFD for wastewater treatment: An overview, *Water Sci. Technol.*, 2016, vol. 74, no. 3, pp. 549–563. https://doi.org/10.2166/wst.2016.249
7. Gebreeyessus, G.D., Status of hybrid membrane–ion–exchange systems for desalination: A comprehensive review, *Appl. Water Sci.* 2019, vol. 9, no. 5, article no. 135, pp. 1–14. https://doi.org/10.1007/s13201-019-1006-9
8. Nikiforov, A.S., Kulichenko, V.V., and Zhikharev, M.M., *Obezvrezhivanie zhidkikh radioaknivnykh otkhodov* (Neutralization of Liquid Radioactive Waste), Moscow: Energoatomizdat, 1985.
9. Zheleznov, V.V. and Vysotskii, V.L., Application of fibrous carbon ferrocyanide sorbents for removing cesium and cobalt from large volumes of sea water, *At. Energy*, 2002, vol. 92, no. 6, pp. 493–500. https://doi.org/10.1023/A:1020270300242
10. El-Shazly, E.A.A., Dakroury, G.A., and Someda, H.H., Sorption of ^{134}Cs radionuclide onto insoluble ferrocyanide loaded silica-gel, *J. Radioanal. Nucl. Chem.*, 2021, vol. 329, no. 1, pp. 437–449. https://doi.org/10.1007/s10967-021-07789-7
11. Watari, K., Imai, K., Ohmomo, Y., Muramatsu, Y., Nishimura, Y., Izawa, M., and Baciles, L.R., Simultaneous adsorption of Cs-137 and I-131 from water and milk on "metal ferrocyanide–anion exchange resin", *J.*

Nucl. Sci. Technol., 1988, vol. 25, no. 5, pp. 495–499. https://doi.org/10.1080/18811248.1988.9733618

12. Mimura, H., Ikarashi, Y., Ishizaki, E., and Matsukura, M., Selective decontamination and stable solidification of Cs-insoluble ferrocyanide by zeolites, *Adv. Sci. Tekhnol.,* 2014, vol. 94, pp. 75–84. doi 10.4028/www.scientific.net/AST.94.75
13. Ikarashi, Y., Mimura, H., Nakai, T., Niibori, Y., Ishizaki, E., and Matsukura, M., Selective cesium uptake behavior of insoluble ferrocyanide loaded zeolites and development of stable solidification method, *J. Ion Exch*., 2014, vol. 25, no. 4, pp. 212–219. https://doi.org/10.5182/jaie.25.212
14. Bykov, G.L., Milyutin, V.V., Ershov, B.G., Korchagin, Yu.P., Gelis, V.M., and Bessonov, A.A., Radiation resistance of a composite ferrocyanide–silica gel sorbent, *Radiochemistry*, 2011, vol. 53, no. 2, pp. 191–195. https://doi.org/10.1134/S1066362211020135
15. Rumyantseva, E.V., Veleshko, A.N., Kulyukhin, S.A., Veleshko, I.E., Shaitura, D.S., Rozanov, K.V., and Dmitrieva, N.A., Preparation and properties of modified spherically granulated chitosan for sorption of ^{137}Cs from solutions, *Radiochemistry*, 2009, vol. 51, no. 5, pp. 496–501. https://doi.org/10.1134/S1066362209050105
16. Egorin, A.M., Didenko, N.A., Kaidalova, T.A., and Zemskova, L.A., Preparation and properties of chitosan-containing ferrocyanide sorbents for the sorption of ^{137}Cs from liquid media, *Radiochemistry*, 2014, vol. 56, no. 3, pp. 275–282. https://doi.org/10.1134/S1066362214030096
17. Lee, J.H. and Suh, D.H., Entropy, enthalpy, and gibbs free energy variations of ^{133}Cs via CO_2-activated carbon filter and ferric ferrocyanide hybrid composites, *Nucl. Eng. Technol.*, 2021, vol. 53, no. 11, pp. 3711–3716. https://doi.org/10.1016/j.net.2021.06.006
18. Gaur, S., Determination of Cs-137 in environmental water by ion-exchange chromatography, *J. Chromatogr. A*, 1996, vol. 733, nos. 1–2, pp. 57–71. https://doi.org/10.1016/0021-9673(95)00906-X
19. Egorin, A., Tokar, E., and Zemskova, L., Chitosan-ferrocyanide sorbent for Cs-137 removal from mineralized alkaline media, *Radiochim. Acta*, 2016, vol. 104, no. 9, pp. 657–661. https://doi.org/10.1515/ract-2015-2536
20. Pereao, O., Uche, C., Bublikov, P.S., Bode-Aluko, C., Rossouw, A., Vinogradov, I.I., Nechaev, A.N., Opeolu, B., and Petrik, L., Chitosan/PEO nanofibers electrospun on metallized track-etched membranes: fabrication and characterization, *Mater. Today Chem.*, 2021, vol. 20, article no. 100416. https://doi.org/10.1016/j.mtchem.2020.100416
21. Vinogradov, I.I., Petrik, L., Serpionov, G.V., and Nechaev, A.N., Composite membrane based on track-etched membrane and chitosan nanoscaffold, *Membr. Membr. Technol.*, 2021, vol. 3, no. 6, pp. 400–410. https://doi.org/10.1134/S2517751621060093
22. Berber, M.R., Current advances of polymer composites for water treatment and desalination, *J. Chem.*, 2020, vol. 2020, article no. 7608423, pp. 1–19. https://doi.org/10.1155/2020/7608423
23. Mchedlishvili, B., Beryozkin, V.V., Oleinikov, V.A., Vilensky, A.I., and Vasilyev, A.B., Structure, physical and chemical properties and applications of nuclear filters as a new class of membranes, *J. Membr. Sci.*, 1993, vol. 79, nos. 2–3, pp. 285–304. https://doi.org/10.1016/0376-7388(93)85122-D
24. RF Patent 2430777, 2011.
25. Artoshina, O.V., Rossouw, A., Semina, V.K., Nechaev, A.N., and Apel, P.Y., Structural and physicochemical properties of titanium dioxide thin films obtained by reactive magnetron sputtering, on the surface of track-etched membranes, *Pet. Chem.*, 2015, vol. 55, no. 10, pp. 759–768. https://doi.org/10.1134/S0965544115100011
26. Mekahlia, S. and Bouzid, B., Chitosan-Copper (II) complex as antibacterial agent: synthesis, characterization and coordinating bond–activity correlation study, *Phys. Procedia*, 2009, vol. 2, no. 3, pp. 1045–1053. https://doi.org/10.1016/j.phpro.2009.11.061
27. Dmitriev, Yu.A., Shipovskaya, A.B., and Kossovich, L.Yu., Influence of the spinning solution characteristics and electroforming parameters on the rate of formation and diameter of fibers from chitosan, *Izv. Vyssh. Uchebn. Zaved., Khim. Khim. Tekhnol.*, 2011, vol. 54, no. 11, pp. 109–112.
28. Khomenko, A.Yu., Popryadukhin, P.V., Bogomolova, T.B., Dobrovol'skaya, I.P., Mamagulashvili, V.G., Shepelev, A.D., Chvalun, S.N., Yudin, V.E., Ivan'kova, E.M., Matrices based on chitosan nanofibers for cell technologies, *Nanotechnol. Russ.*, 2013, vol. 8, no. 9, pp. 639–643. https://doi.org/10.1134/S1995078013050054
29. Li, B., Shan, C.-L., Zhou, Q., Fang, Y., Wang, Y.-L., Xu, F., Han, L.-R., Ibrahim, M., Guo, L.-B., Xie, G.-L., and Sun, G.-C., Synthesis, characterization, and antibacterial activity of cross-linked chitosan-glutaraldehyde, *Mar. Drugs*, 2013, vol. 11, no. 5, pp. 1534–1552. https://doi.org/10.3390/md11051534
30. Panarin, E.F., Nud'ga, L.A., Petrova, V.A., Bochek, A.M., Gofman, I.V., Lebedeva, M.F., Blinova, M.I., Spichkina, O.G., Yudintseva, N.M., and Pinaev, G.P., Matrices for calculating human skin cells based on natural polysaccharides—chitin and chitosan, *Kletochnaya Transplantologiya, Tkanevaya Inzh.,* 2009, vol. 4, no. 3, pp. 42–46.
31. Liu, A. and Berglund, L.A., Clay nanopaper composites of nacre-like structure based on montmorrilonite and cellulose nanofibers—Improvements due to chitosan addition, *Carbohydr. Polym.*, 2012, vol. 87, no. 1, pp. 53–60. https://doi.org/10.1016/j.carbpol.2011.07.019
32. Gustova, M.V., Vinogradov, I.I., Gustova, N.S., and Nechaev, A.N., Studies on cesium sorption by modified track membrane, *Trudy X Rossiiskoi konferentsii s mezhdunarodnym uchastiem "Radiokhimiya-2022"* (Proc. X Ross. Conf. Int. Participation "Radiochemistry 2022"). S.-Peterb., 2022, p. 86.
33. Berezkin, V.V., Vasiliev, A.B., Tsyganova, T.V., Mchedlishvili, B.V., Apel', P.Yu., Orelovich, O.L., Oleynikov, V.A., Prostyakova, A.I., and Khokhlova, T.D., Asymmetrical track-etched membranes: Surface and operational properties, *Membrany*, 2008, no. 4, pp. 3–8.

34. Vinogradov, I.I., Eremin, P.S., Poddubikov, A.V., Gil'mutdinova, I.R., and Nechaev, A.N., Bioplastic material based on ion-track wound coatings and chitosan nano-scaffold, *Biotekhnologiya*, 2021, vol. 37, no. 5, pp. 55–60.
35. Rigamonti, R., Structure of cupriferrocyanides I. Copper ferrocyanide and potassium copper ferrocyanide, *Gazz. Chim. Ital.*, 1937, vol. 67, pp. 137–146.
36. Loos-Neskovic, C., Ayrault, S., Badillo, V., Jimenez, B., Garnier, E., Fédoroff, M., Jones, D.J., and Merinov, B., Structure of copper-potassium hexacyanoferrate (II) and sorption mechanisms of cesium, *J. Solid State Chem.*, 2004, vol. 177, no. 6, pp. 1817–1828. https://doi.org/10.1016/j.jssc.2004.01.018
37. Zotkin, M.A., Vikhoreva, G.A., Kechek'yan, A.S., Thermal modification of chitosan films in the form of salts with various acids, *Vysokomol. Soedin.*, 2004, vol. 46, no. 2, pp. 359–363.
38. Ojwang, D.O., Grins, J., Wardecki, D., Valvo, M., Renman, V., Häggström, L., Ericsson, T., Gustafsson, T., Mahmoud, A.P., Hermann, R.P., and Svensson, G., Structure characterization and properties of K-containing copper hexacyanoferrate, *Inorg. Chem.*, 2016, vol. 55, no. 12, pp. 2924–5934. https://doi.org/10.1021/acs.inorgchem.6b00227
39. Malakhova, I., Privar, Yu., Parotkina, Yu., Mironenko, A., Eliseikina, M., Balatskiy, D., Golikov, A., and Bratskaya, S., Rational design of polyamine-based cryogels for metal ion sorption, *Molecules*, 2020, vol. 25, no. 20, article no. 4801, pp. 1–17. https://doi.org/10.3390/molecules25204801
40. Tananaev, I.V., Seifer, G.B., Kharitonov, Yu.Ya., Kuznetsov, V.G., and Korol'kov, A.P., *Khimiya ferrotsianidov* (Chemistry of Ferrocyanides), Moscow: Nauka, 1971.
41. Panasyugin, A.S., Tsyganov, A.R., Masherov, N.P., and Grigor'ev, S.V., Adsorption structure properties of intercalated cobalt ferrocyanides, *Tr. Beloruss. Gos. Univ., Ser. 2*, 2018, vol. 2, no. 1, pp. 128–134.
42. Guibal, E., Interactions of metal ions with chitosan-based sorbents: A review, *Sep. Purif. Technol.*, 2004, vol. 38, no. 1, pp. 43–74. https://doi.org/10.1016/j.seppur.2003.10.004
43. Lima, I.S. and Airoldi, C., Interaction of copper with chitosan and succinic anhydride derivative—a factorial design evaluation of the chemisorption process, *Colloids Surf., A*, 2003, vol. 229, nos. 1–3, pp. 129–136. https://doi.org/10.1016/S0927-7757(03)00310-8
44. Gellings, P.J., Structure of some hexacyanoferrates (II) of the type $K_2M_{II}Fe(CN)_6$, *Z. Phys. Chem.*, 1967, vol. 54, pp. 296–301. https://doi.org/10.1524/zpch.1967.54.5_6.296
45. Artoshina, O.V., Milovich, F.O., Rossouw, A., Gorberg, B.L., Iskhakova L.D., Ermakov, R.P., Semina, V.K., Kochnev, Yu.K., Nechaev, A.N., and Apel, P.Y., Structure and phase composition of thin TiO_2 films grown on the surface of metallized track-etched polyethylene terephthalate membranes by reactive magnetron sputtering, *Inorg. Mater.*, 2016, vol. 52, no. 9, pp. 945–954. https://doi.org/10.1134/S0020168516080021
46. Avramenko, V., Bratskaya, S., Zheleznov, V., Sheveleva, I., Voitenko, O., and Sergienko, V., Colloid stable sorbents for cesium removal: Preparation and application of latex particles functionalized with transition metals ferrocyanides, *J. Hazard. Mater.*, 2011, vol. 186, nos. 2–3, pp. 1343–1350. https://doi.org/10.1016/j.jhazmat.2010.12.009

Translated by E. Glushachenkova